TECTONICS, VOL. 15, NO. 2, PAGES, 456-471, APRIL 1996

Crustal and upper mantle velocity structure of the Salton Trough, southeast California

Tom Parsons and Jill McCarthy
U.S. Geological Survey, Menlo Park, California

Abstract. This paper presents data and modelling results from a crustal and upper mantle wide-angle seismic transect across the Salton Trough region in southeast California. The Salton Trough is a unique part of the Basin and Range province where mid-ocean ridge/transform spreading in the Gulf of California has evolved northward into the continent. In 1992, the U.S. Geological Survey (USGS) conducted the final leg of the Pacific to Arizona Crustal Experiment (PACE). Two perpendicular models of the crust and upper mantle were fit to wide-angle reflection and refraction travel times, seismic amplitudes, and Bouguer gravity anomalies. The first profile crossed the Salton Trough from the southwest to the northeast, and the second was a strike line that paralleled the Salton Sea along its western edge. We found thin crust (~21-22 km thick) beneath the axis of the Salton Trough (Imperial Valley) and locally thicker crust (~27 km) beneath the Chocolate Mountains to the northeast. We modelled a slight thinning of the crust further to the northeast beneath the Colorado River (~24 km) and subsequent thickening beneath the metamorphic core complex belt northeast of the Colorado River. There is a deep, apparently young basin (~5-6 km unmetamorphosed sediments) beneath the Imperial Valley and a shallower (~2-3 km) basin beneath the Colorado River. A regional 6.9-km/s layer (between ~15-km depth and the Moho) underlies the Salton Trough as well as the Chocolate Mountains where it pinches out at the Moho. This lower crustal layer is spatially associated with a low-velocity (7.6-7.7 km/s) upper mantle. We found that our crustal model is locally compatible with the previously suggested notion that the crust of the Salton Trough has formed almost entirely from magmatism in the lower crust and sedimentation in the upper crust. However, we observe an apparently magmatically emplaced lower crust to the northeast, outside of the Salton Trough, and propose that this layer in part predates Salton Trough rifting. It may also in part result from migration of magmatic spreading centers associated with the southern San Andreas fault system. These spreading centers may have existed east of their current locations in the past and may have influenced the lower crust and upper mantle to the east of the current Salton Trough.

Introduction

The primary purpose of this paper is to show data from and provide an interpretation of a whole crustal and upper mantle long-offset seismic experiment conducted across the Salton Trough in southeastern California in 1992 by the U.S. Geological Survey (USGS) as the final part of the Pacific to Arizona Crustal Experiment (PACE) (Figure 1) (see *McCarthy et al.* [1991], *Wilson et al.* [1991], *Wolf and Cipar* [1993], *McCarthy and Parsons* [1994], for background on PACE). The refraction data interpreted here sample the crust and upper mantle of the incipient ocean margin forming in the Salton Trough as the Gulf of California apparently migrates north. These profiles cross a complex region where oceanic spreading gives way to primarily transform motion along the southern end of the San Andreas fault system.

The most comprehensive active-source seismic study of the Salton Trough to date was that of *Fuis et al.* [1984]. This experiment was carried out in 1979 by the USGS and provided detailed velocity structure of the upper and middle crust throughout the Salton Trough. No deep-crustal or upper mantle phases (such as *PmP* or *Pn*) were recorded, and the deep crust was modelled using Bouguer gravity data. The seismic models of *Fuis et al.* [1984] showed a thick (up to 6 km) unmetamorphosed sedimentary package overlying metamorphic basement, which was shown to be underlain by high-velocity (7.2 km/s) mafic rocks. This sequence was interpreted to have resulted from simultaneous lower crustal mantle-derived magmatic intrusion with high rates of sedimentation from above, which created an intervening metamorphic layer. This type of model is also compatible with heat-flow models [e.g., *Lachenbruch et al.*, 1985], the isotope geochemistry of Salton Trough basalts [e.g., *Herzig and Jacobs*, 1994], and comparative rift studies [e.g., *Nicolas*, 1985]. The uppermost mantle beneath the Salton Trough (70-100 km) shows a 3-4% reduction in *P* wave velocity as compared with the average velocity of the southern California upper mantle [*Humphreys and Clayton*, 1990]. This low-velocity zone is asymmetric about the Salton Trough and extends east toward the Colorado River.

There are some intriguing questions associated with the Salton Trough. For example, why does large-magnitude extension there create deep basins instead of the mountainous Miocene core complex terranes that outcrop along the PACE transect to the northeast (Figure 1)? Is the Salton Trough an example of completely new crustal generation (magmatic addition from below, sedimentary addition from above) as suggested by *Fuis et al.* [1984], *Lachenbruch et al.* [1985], and *Nicolas* [1985]; if so, how does such new crust compare with more typical Phanerozoic crust? The Salton Trough is suggested to be the northern extension of mid-ocean style spreading in the Gulf of California, yet it is relatively amagmatic at the surface; where does the magma stall and why? We present a crustal model and address these questions in the discussion that follows.

This paper is not subject to U.S. copyright. Published in 1996 by the American Geophysical Union.

Paper number 95TC02616.

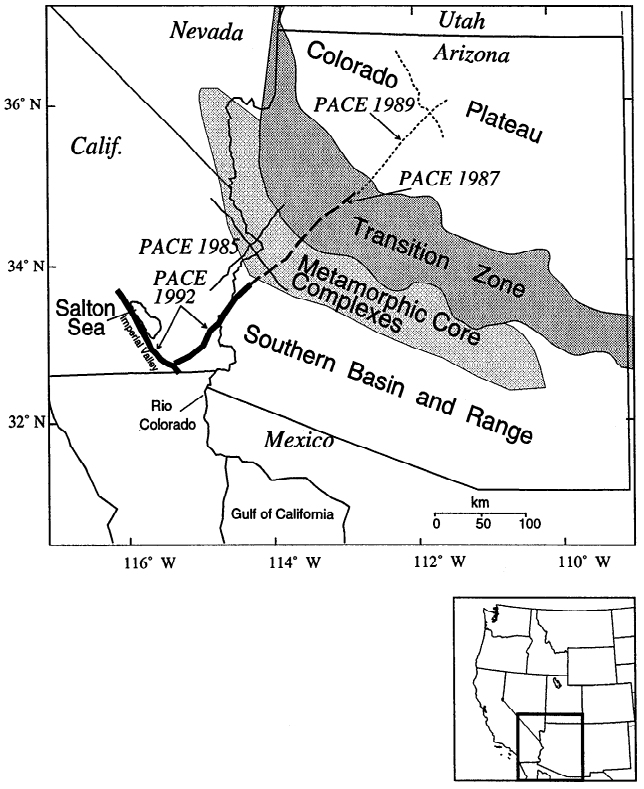

Figure 1. Locations of the U.S. Geological Survey (USGS) Pacific to Arizona Crustal Experiment (PACE) profiles from the 1985 to the 1992 experiments. The major tectonic provinces discussed are shown.

Geological and Geophysical Background

The Salton Trough results from northward progression of the enlarging Gulf of California [e.g., *Larson et al.*, 1968; *Moore and Buffington*, 1968; *Elders et al.*, 1972; *Crowell*, 1989; *Lonsdale*, 1989; *Larsen and Reilenger*, 1991]. The initial opening of the Gulf of California occurred about 12-10 Ma, shortly after subduction ceased along the continental margin of Mexico [e.g., *Lonsdale*, 1989; *Stock and Hodges*, 1989]. The Gulf of California has been characterized as a series of en echelon right-lateral transform faults that formed in response to Pacific-North American relative motion and were linked initially by pull-apart basins that matured into oceanic spreading centers [*Lonsdale*, 1989]. The Salton Trough apparently represents a present-day onshore analog to these Gulf of California evolving spreading centers [e.g., *Elders et al.*, 1972]. The Cerro Prieto, Imperial, Brawley, and San Andreas faults form an en echelon series of east stepping right-lateral transforms linked by pull aparts named the Cerro Prieto, Brawley, and Salton Buttes spreading centers by *Elders et al.*, [1972] (Figure 2). These spreading centers have probably not been stable through time and have likely changed position more than once; for example, the parallel Sand Hills and Algodones faults may represent fossil transforms or spreading centers parallel to but ~45 km east of the Imperial fault [e.g., *Lachenbruch et al.*, 1985; *Lonsdale*, 1989] (Figure 2). Farther northeast (farthest extent is ~60 km northeast of the Imperial fault; Figure 2), smaller late Cenozoic strike-slip faults are also known from surface exposures, and these likely represent parts of the evolving transform system (R. Tosdal, personal communication, 1995).

The Imperial Valley-Salton Trough is highly active seismically. Most of the seismicity occurs along the Imperial and Brawley fault zones [e.g., *Larsen and Reilinger*, 1991]. Large quakes have occurred on the Imperial fault in 1940 (M_S 7.1) and in 1979 (M_S 6.9). *Larsen and Reilinger* [1991] suggest based on geodetic, seismic, and heat-flow data that the Imperial and Brawley fault systems are young (3000-100,000 years old) and have migrated northwest into the Imperial Valley. The southernmost part of the active San Andreas fault extends northwest from the southeast corner of the Salton Sea (Figure 2). A palinspathic reconstruction indicates that displacement on the southern part of the San Andreas fault began about 10 Ma, with about 60 km of right-lateral displacement occurring before 5 Ma and 240 km of right slip occurring between 5 Ma and the present [*Dillon and Ehlig*, 1993]. The Clemens Well fault, lying to the east of the San Andreas fault and the Orocopia Mountains (Figure 2), has been proposed as an early mid-Miocene strike-slip fault that accommodated up to 110 km of right-lateral displacement [*Powell*, 1993].

Heat Flow and Magmatism

High heat flow (~140 mW m^{-2}, locally can exceed 200 mW m^{-2}) characterizes the Salton Trough and surrounding regions [*Lachenbruch et al.*, 1985]. High heat flow is concentrated primarily within the basins of the Salton Trough, while the adjacent crystalline mountain ranges have heat-flow values more near the southern Basin and Range norm. Heat-flow data [*Lachenbruch et al.*, 1985] limit the extension rate in the Salton Trough to have been about 20-50%/m.y. distributed across a zone about 150 km wide during the past 4-5 m.y. *Lachenbruch et al.* [1985] proposed that extension was accomplished by lower crustal growth through emplacement of gabbro and upper crustal growth through sedimentation.

While localized upper crustal melting is suggested from the high heat-flow values in the Salton Trough [*Swanberg*, 1983], a relatively small volume of Cenozoic volcanic rocks has been extruded to the surface in the region. Eruptions are thought to have occurred in three phases, a 25-to 22-m.y.-old calc-alkaline series of volcanic rocks in the Chocolate Mountains, a basaltic series (22-13 m.y. old) related to Miocene Basin and Range extension (also found east of the San Andreas fault in the Chocolate Mountains), and recent (~16,000 years old) bi-modal (basalt-rhyolite) rocks of the Salton Buttes which define the Salton Buttes spreading center that connects the Brawley and San Andreas fault zones at the southern end of the Salton Sea [*Korsch*, 1979] (Figure 2). Isotopic and geochemical compositions of (<4 Ma) Salton Trough basalts and (~13 Ma) basalts from the Chocolate Mountains are consistent with two distinct phases of extension and mafic magmatism [*Herzig and Jacobs*, 1994]. Initial thinning of continental crust occurred in a mid-Miocene extensional phase that was widespread in the region to the northeast; half grabens filled with clastic rocks and alkaline basalts record this episode [*Crowe*, 1978]. Final rifting initiated ~4 Ma and was completed in the Holocene northeast of the present-day Salton Trough.

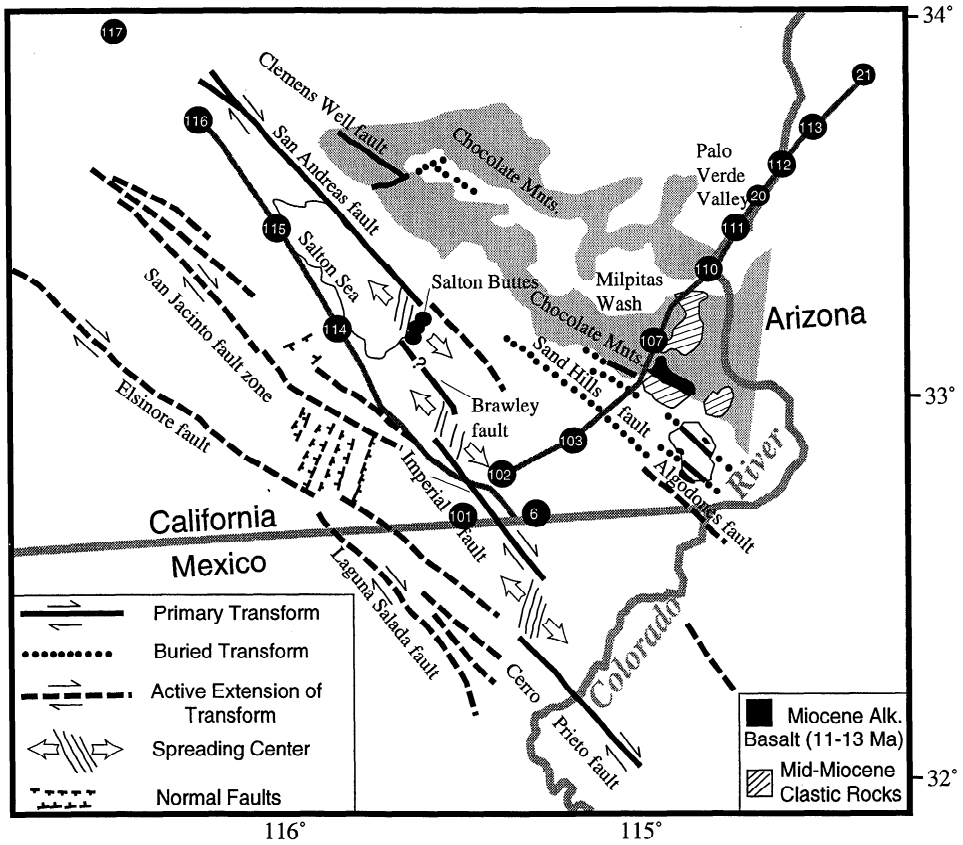

Figure 2. Active faults and spreading centers in the Salton Trough region. The locations of the seismic profiles and some shot point locations are shown. The Salton Trough lies in a domain of east-stepping right-lateral transforms bounded by apparent crustal spreading centers [*Lonsdale,* 1989]. These structures are on-land analogs to the spreading occurring in the Gulf of California.

Experiment Design

Two refraction/wide-angle reflection profiles were acquired during the 1992 PACE experiment. The first profile, referred to as the transect profile, was oriented NE-SW and extended 150 km from the Colorado River, southwest to the Mexico-United States border. The transect profile connects with the main PACE 1987-1989 profiles that extend onto the Colorado Plateau (Figure 1). Instruments were spaced every 350 m, and a total of 27 shots were fired from 22 independent shot point locations (Figure 2). Two of these shots were offset to the southwest of the recording line, and one was offset to the northeast. The second refraction profile, referred to as the Salton Sea profile, was oriented NW-SE and extended 150 km from the United States-Mexico border to La Quinta, California, along the west side of the Salton Sea. Instruments were spaced every 350 m. There were a total of 5 shots fired into this receiver array, with the northwestern-most shot being offset from the spread (Figure 2). This profile reoccupied and extended a line recorded by the USGS in 1979 [*Fuis et al.*, 1984]; two of the five shots on this profile were co-located with shots fired into the earlier profile. The other three shots were located further to the northwest and were designed to provide greater shot-receiver offsets for deep crustal structure beneath the Salton Trough.

Description of the Data

The crustal and upper mantle velocity structure of the Salton Trough was derived from four major seismic phases: direct and refracted arrivals from the upper crust (*Pg*) and upper mantle (*Pn*) and reflected phases from a middle crustal horizon (*PiP*) and the Moho (*PmP*). The middle crustal reflection (*PiP*) was observed on six shots on the transect profile and provided primary control for the velocity of the upper to middle crust. The middle crustal reflector was observed on four shots on the Salton Sea profile. The reflection from the crust-mantle boundary (*PmP*) was observed on 11 shots on the transect profile and three shots on the Salton Sea profile. This phase provided control on estimates of lower crustal velocity and crustal thickness. *Pn* refractions were observed on seven long-offset shots on the transect profile and provide control on upper mantle velocities across the Salton Trough. The bulk of the *Pn* refractions observed came from shots on the southwest part of the line, and only a small segment of a *Pn* refraction was observed in a reversing direction from shots to the northeast. Determining upper mantle velocities from essentially unreversed *Pn* refractions requires that the crustal thickness and velocity be known. Thus the upper mantle velocities we report here are subject to the same uncertainties as our crustal thickness and velocity estimates.

The overall quality and signal-to-noise ratio of the 1992 PACE data were as good or better than those of the data collected along the PACE profiles in 1985, 1987 [e.g., *McCarthy et al.*, 1991], and 1989 [e.g., *Wolf and Cipar*, 1993; T. Parsons et al., The crustal structure of the Colorado Plateau, Arizona: Application of new long-offset seismic data analysis methods, submitted to *Journal of Geophysical Research*, 1995; hereinafter referred to as Parsons et al., submitted manuscript, 1995]. Unequivocal reflections from the Moho (*PmP*) were observed on 14 shots as bright phases. Less obvious reflected events were observed from a middle crustal horizon which tended to cause complicated reflections at long offsets (more discussion on this provided in subsequent sections). The direct and refracted *Pg* arrivals carried to the end of the profiles on all shots and allowed us to define the shapes of the basins along the transect profile. On the Salton Sea profile, only five shots were detonated, causing more limited upper crustal coverage. Thus the upper crustal velocity structure is much better resolved on the transect profile than on the Salton Sea profile. Clear but relatively low amplitude *Pn* phases were observed beginning at about 110 km offset mostly from shots detonated on the southwest part of the transect profile.

Modeling Refraction and Reflection Travel Times

We apply relatively new techniques to model long-offset data (discussed in detail by Parsons et al., submitted manuscript, 1995) that rely on travel-time computations using finite-difference algorithms developed by *Vidale* [1988, 1990]. We modelled the upper crust by inverting first arrival times based on a modification of the method of *Ammon and Vidale* [1993] capable of imaging media containing strong velocity variations. Once we acquired a solution for the upper crustal velocity structure, we applied a second technique to model secondary arrivals such as wide-angle reflections from middle crustal horizons and the Moho. This method utilizes *Vidale*'s [1990] algorithm as developed by *Hole* [1993] and *Hole and Zelt* [1995] and computes first-arrival times from a point source down to a reflecting boundary, where the incident times are stored. The incident travel times are then used as a source to propagate the reflected wave upward though the model. The reflector position and velocities are altered in a forward manner until the residuals between picked travel times from the data and calculated travel times are minimized to within the picking error. The output is a gridded velocity field. We then use the gridded velocity field as input to a finite-difference solution of the acoustic wave equation to model amplitudes of refracted and reflected phases. Our gridded velocity model is also converted into a density model, and fit to the observed Bouguer gravity data.

First-Arrival Travel-Time Inversion for Upper Crustal Velocity Structure

We inverted 5580 *Pg* travel-time observations from 21 shots along the transect profile (Figure 3) for upper crustal velocity structure. Another 856 observations from five shots were inverted to find the velocity structure on the Salton Sea profile. We used a one-dimensional starting velocity model for the better covered transect profile and extended the final transect model from the tie point for use as the starting model for the Salton Sea profile. The inversion models were parameterized using horizontal and vertical velocity cell widths of 0.5 km. To maintain accuracy, a uniform grid point spacing of 100 m was employed for the travel-time calculations. Figure 3 contains the results of our inversion for the transect model. The final velocity model was obtained after five iterations. The travel-time RMS residuals decreased from 0.28 s (for the one-dimensional starting model) to 0.08 s for the final model. We estimate that our picking error is about 0.1 s for all phases on the PACE 1992 data and fit all models to within that error limit.

The primary feature resolved by the travel-time inversion was the deep sedimentary basin beneath the Salton Trough (Figure 3). We found velocities appropriate for unmetamorphosed sedimentary rocks ($\leq$ 5.0 km/s as defined by *Fuis et al.* [1984]) persisting to depths of ~5.0 km beneath the Imperial Valley. Northeast of the sedimentary basin beneath the Imperial Valley, higher velocities were observed nearer to the surface beneath the Chocolate Mountains where rocks with velocities of 5.0 km/s are about 1.5 km beneath the surface. These velocity structures are in good agreement with the nearest profiles (1E-2W) of *Fuis et al.* [1984] that crossed the Salton Trough. They observed velocities of 5.5 km/s at ~5.0 km above a 6.0 km/s basement beneath the Imperial Valley, and they also modelled a thinning of the basin to less than 1 km beneath the Chocolate Mountains to the east. Northeast of the Chocolate Mountains we modelled another basin that is associated with the Milpitas Wash and Palo Verde Valley. This basin is about 3 km thick and is occupied by the Colorado River on its northeastern edge. The original one-dimensional starting model is preserved southwest of shot point 101 where there was no coverage (Figure 3). The distinct vertical velocity boundary shown at about km 55 in the model probably results from the reduction in coverage southwest of that point. The Salton Sea profile upper crust was essentially unchanged by the inversion from the starting model extrapolated from the transect model at the tie point, probably a result of the limited upper crustal coverage. The reader is directed to the comprehensive study of the upper crust and basin structure by *Fuis et al.* [1984] for more detailed discussion. A complete discussion on the tomographic methods applied here is given by Parsons et al. (submitted manuscript, 1995).

Finite-Difference Reflection Travel Times

A Middle-Crustal Horizon

Ten shots recorded in the Salton Trough generated middle crustal reflections from a boundary approximately 13-15 km deep. These reflections tend to be weak at near offsets but can become quite strong at longer offsets where they merge with the *PmP* reflections (e.g., Figures 4 and 5) Because these reflections are either weak or difficult to discern from the *PmP* reflections at longer offsets, we first attempted a simple model of the crust without a high-velocity lower crustal layer by picking all the bright secondary phases as *PmP* reflections. However, this approach failed to converge on a consistent solution because apparent reversing reflections at similar offsets did not have the same reciprocal times. We found that the most complicated reflections could be picked as two phases

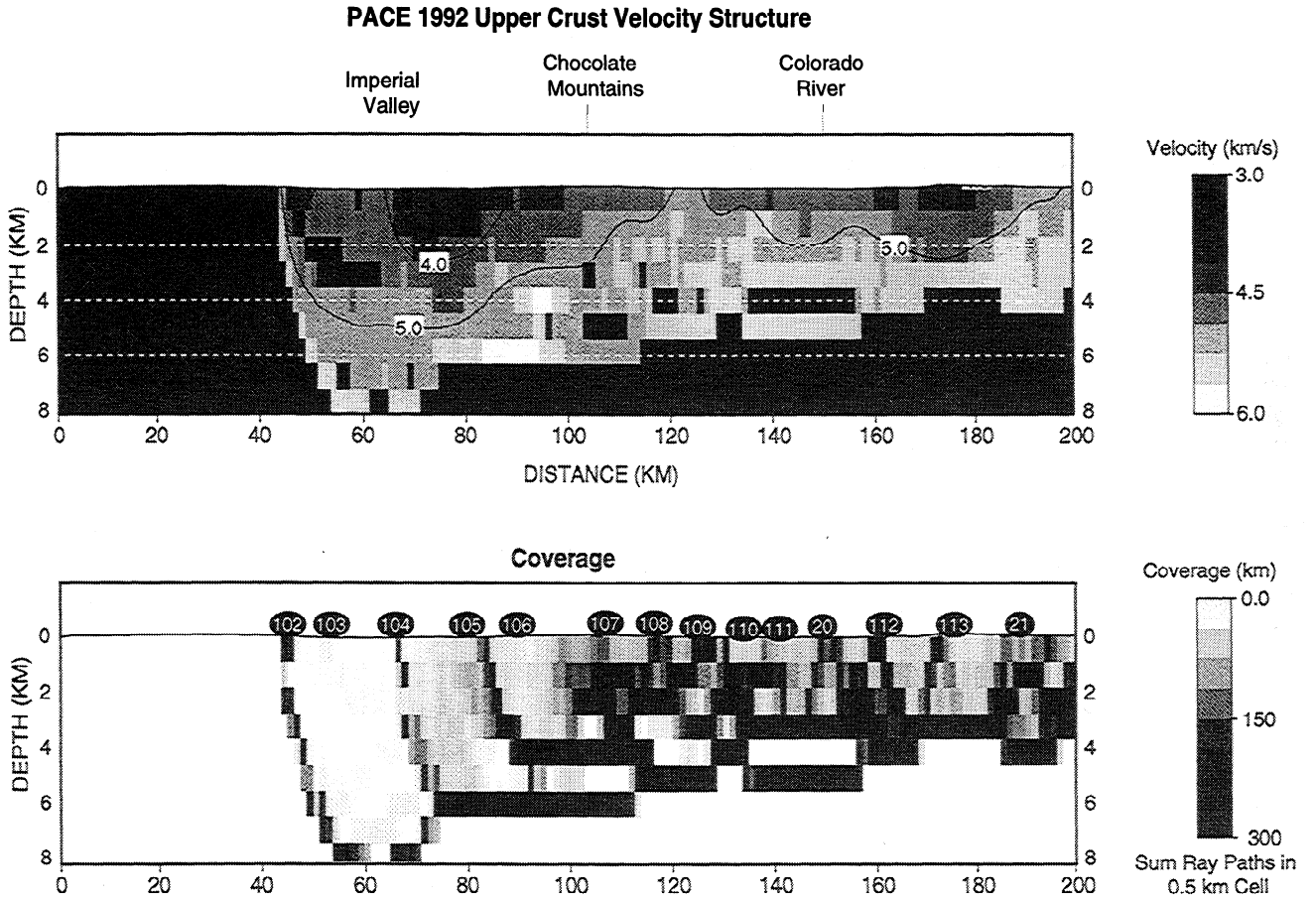

Figure 3. Upper crustal velocity model derived from inversion of travel times of direct and refracted *Pg* arrivals; data from the PACE 1992 experiment were combined with data from PACE 1987 (Figure 1) to increase coverage. Velocity is contoured in kilometers per second. The major upper crustal features resolved are the deep (~5-6 km/s) sedimentary basin beneath the Imperial Valley and a thinner basin (~3 km deep) associated with the Palo Verde Valley that contains the Colorado River. Between the two basins, higher velocities are found at shallow depth beneath the Chocolate Mountains.

and that reciprocity could be achieved with reversing shots if the later phases were attributed to Moho reflections and the earlier phases to middle-crustal reflections. A further complication in the data is that this effect was only observed southwest of km 115 in our model. We thus found that the best fit model would be one in which a relatively high velocity layer exists beneath the Salton Trough to the southwest but fades or pinches out to the northeast (Figure 6). The high amplitudes (modelled in a subsequent section) of the middle-crustal reflections and the curvature of the *PmP* reflections limit the lower crustal layer to be of high velocity (~6.9 km/s). In Figure 7, close-ups of reflections from northeast of the pinch-out (sp 21) and one from southwest of the pinch-out (sp 111) are shown; the difference is especially apparent at ~75 km offset where on sp 111, a complex reflection (*PiP*) arrives about 1 s behind *Pg*. In contrast, the *PmP* reflection on sp 21 arrives ~2 s behind the *Pg* phase; if both of these reflections (sp 111 and sp 21) are treated as *PmP*, this difference in arrival time would require 8-10 km of crustal thinning between these two shots (~40 km), which cannot be fit by the 10 other shots that generated *PmP* reflections.

The lateral resolution of wide-angle reflection modelling is controlled by the ~10-km-width of the Fresnel Zone at depth. That level of resolution limits our ability to locate the position and shape of a pinch-out in the lower crustal layer. A piggyback vertical incidence reflection experiment was carried out by Rice University that collected about 40 km of data from km 90 to km 130 (S. P. Larkin et al., The RISC seismic experiment: Images of deterministic and stochastic structures in the Salton Trough/Basin and Range transition zone and constraints on magmatism during rifting, submitted to *Journal of Geophysical Research*, 1995; hereinafter referred to as Larkin et al., submitted manuscript, 1995) (shown as line drawings on Figure 6). These data show a series of discontinuous dipping reflection patterns that begin at about 15 km depth and dip toward the Moho. High-amplitude diffractions were observed where the dipping reflectivity merges with the Moho reflections; these diffractions were interpreted as resulting from the edge of a significant lateral discontinuity that might likely correspond to the edge of the high-velocity lower crustal layer (Larkin et al., submitted manuscript, 1995). We applied this higher-resolution view of the geometry of an

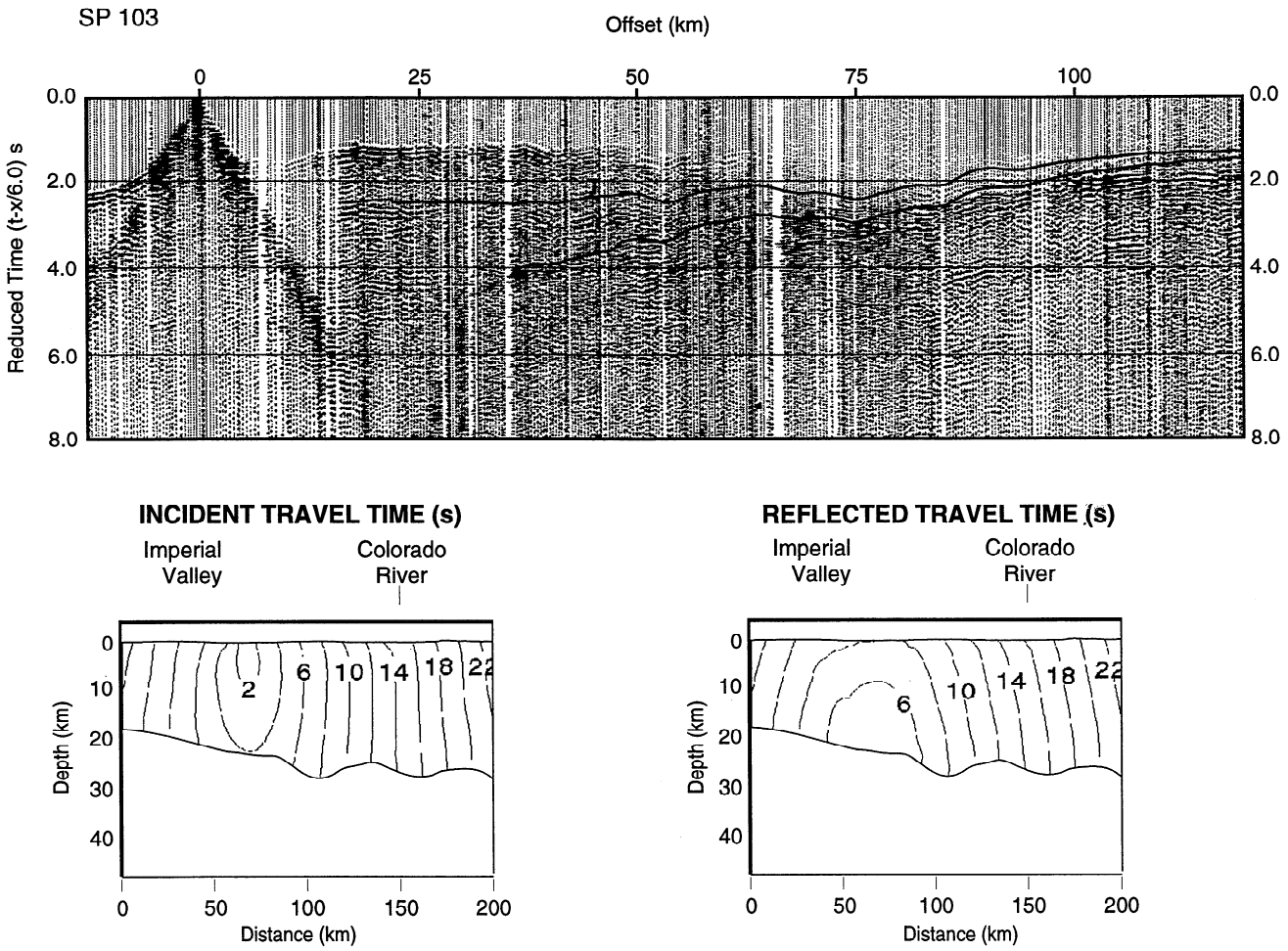

Figure 4. Data plot of shot point 103 on the transect profile (see Figure 2 for the location of this and subsequent shots) with the calculated travel-time curves for the *PmP* and *PiP* reflections superimposed. Contours of incident and reflected travel times through the crustal velocity model are shown below. These contours can be thought of as the instantaneous location of the wavefront at a given time. Seismic rays are lines perpendicular to the travel-time contours at any point.

apparent pinch-out of high-velocity rocks to our wide-angle reflection modelling and found that it fit well with both travel-time and amplitude modelling.

We modelled the velocities in the middle crust between the base of the inverted upper crustal velocity model and the top of the middle-crustal reflector (6.1-6.25 km/s) initially by extending the velocity model from the adjoining PACE 1987 profile to the southwest. These velocities achieved a reasonable fit to the travel times of the middle-crustal reflection where observed. At the northeast end of the line we observed reflections from the lower-crustal layer modelled by *McCarthy et al.* [1991] (6.35 km/s) that underlies the Whipple and Buckskin-Rawhide metamorphic core complexes. Reflections recorded from shots 20 and 21 to the southwest allow us to model the shape of this reflector to about km 155 in the model (Figure 8). Beyond that point to the southwest, the shape of this reflector is speculative (dashed lines on Figure 6), and the relationship between this horizon and the pinch-out of high-velocity rocks at km 115 is unknown. Beneath the Imperial Valley the deepest part of the basin reaches to within 5 km of the top of the high-velocity lower crust. Thus the 6.1-6.25 km/s middle crust of the metamorphic core complexes is thinned dramatically from 20 km thick to only 5 km thick beneath the Imperial Valley.

On the Salton Sea profile, four shots recorded weak reflections from the middle crustal horizon. We encountered similar reciprocity problems as on the transect profile when we attempted to model the Salton Sea line without a high-velocity lower crustal layer. Shots 115 and 116 did not record Moho reflections, only reflections from the middle crust (Figure 8). We modelled a slight rise in the middle crustal reflector between km 40 and km 80 on the Salton Sea profile (Figure 6) to fit reflections from shots 6 and 115 (Figure 8). We view this interpretation as tentative because of uncertainties in the upper crustal velocity structure and the wide shot spacing.

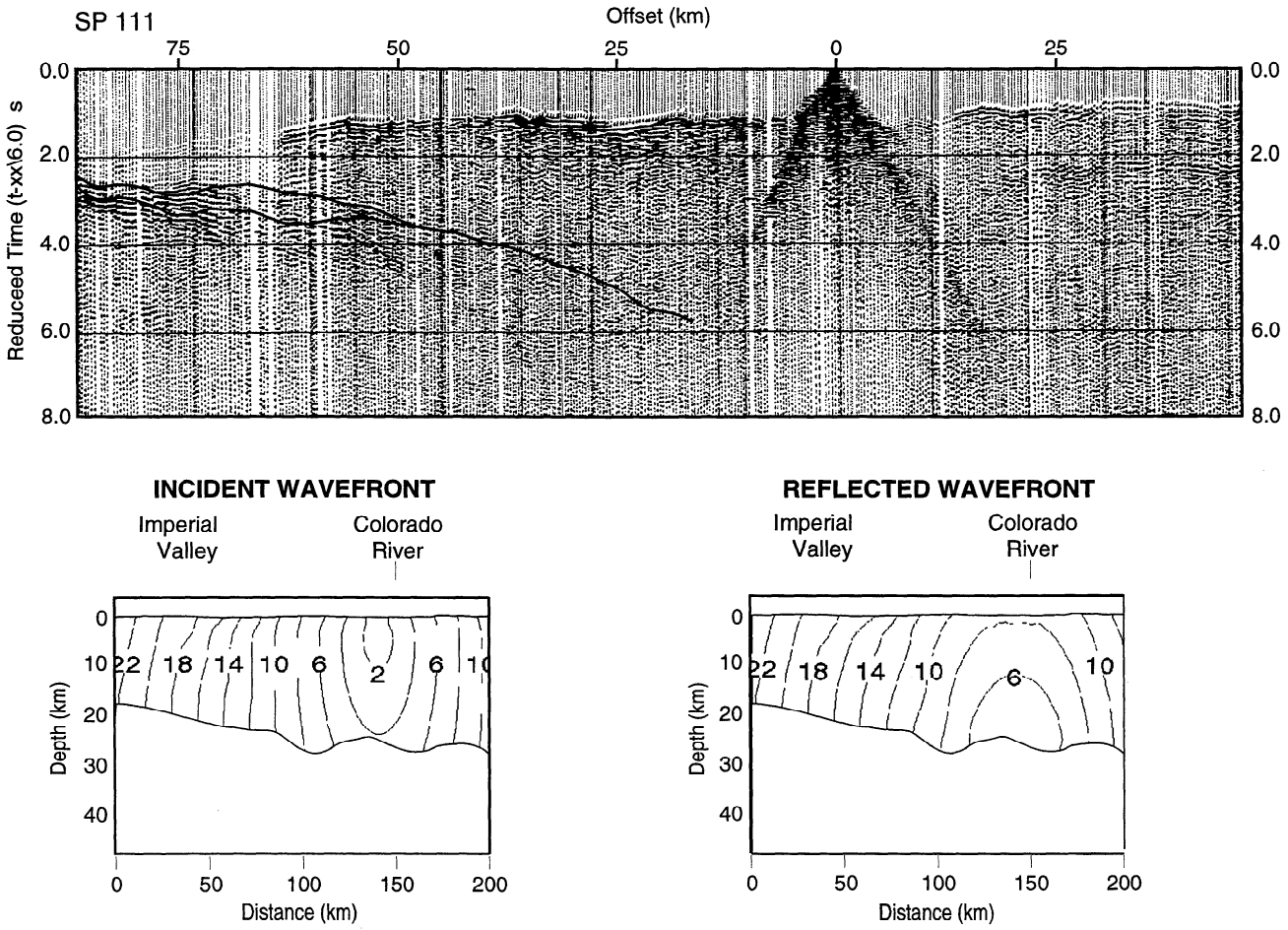

Figure 5. Data plot of shot point 111 on the transect profile with calculated travel-time curves for the *PmP* and *PiP* reflections superimposed. Contours of calculated incident and reflected travel times for the *PmP* reflection are shown below.

The Moho and Whole-Crustal Thickness

The crustal thickness along the transect profile was modelled by reversing *PmP* reflections from 11 shots (Figure 8). The crust beneath the Salton Trough-Imperial Valley is thin at 20-21 km and gradually thickens to a maximum of 27 km beneath the Chocolate Mountains (Figure 6). Northeast of the Chocolate Mountains the crust thins slightly to 23-24 km beneath the Colorado River before it begins to thicken again beneath the core complexes to the northeast [*McCarthy et al.*, 1991]. We fit a uniform 22-km-thick crust to the three shots that recorded Moho reflections on the Salton Sea profile (Figure 6) but recognize the possibility of complications in crustal structure that are beyond what we can resolve given the sparse shot coverage in this model (Figure 8).

Velocities in the lower crust were fit by matching curvature of *PmP* reflections and separation between the middle-crustal reflections and *PmP* reflections. These velocities were also tested independently through amplitude modelling. We found that applying the best fit lower crustal velocities that were observed across the rest of the PACE profiles (6.5-6.6 km/s) failed to fit the PACE 1992 data. We thus experimented with a variety of high and low velocities in this layer and found that a ~6.9-km/s velocity provided the best overall fit. Northeast of the pinch-out of the high velocity layer we modelled the lower crust with slow velocities (6.25-6.35 km/s) because the wide-angle and vertical-incidence data do not show evidence of significant structure on the Moho. These low velocities compare with the 6.35 km/s layer that underlies the metamorphic core complexes to the northeast [*McCarthy et al.*, 1991].

Amplitude Models From Finite-Difference Solutions of the Acoustic Wave Equation

Our interpretation that the wide-angle reflections that bottom beneath the Imperial Valley and Chocolate Mountains consist of two overlapping phases (*PiP* and *PmP*) can be tested by amplitude modelling. Acoustic and elastic wave-equation simulations enable two-dimensional input velocity models that can include gridded upper crustal velocity models generated by travel-time inversions, allowing the effects of lateral near-surface strong velocity contrasts and dipping structures to be modelled. This could become important since scattering effects and reverberations associated with shallow velocity structures might wrongly be attributed to deep interlayering.

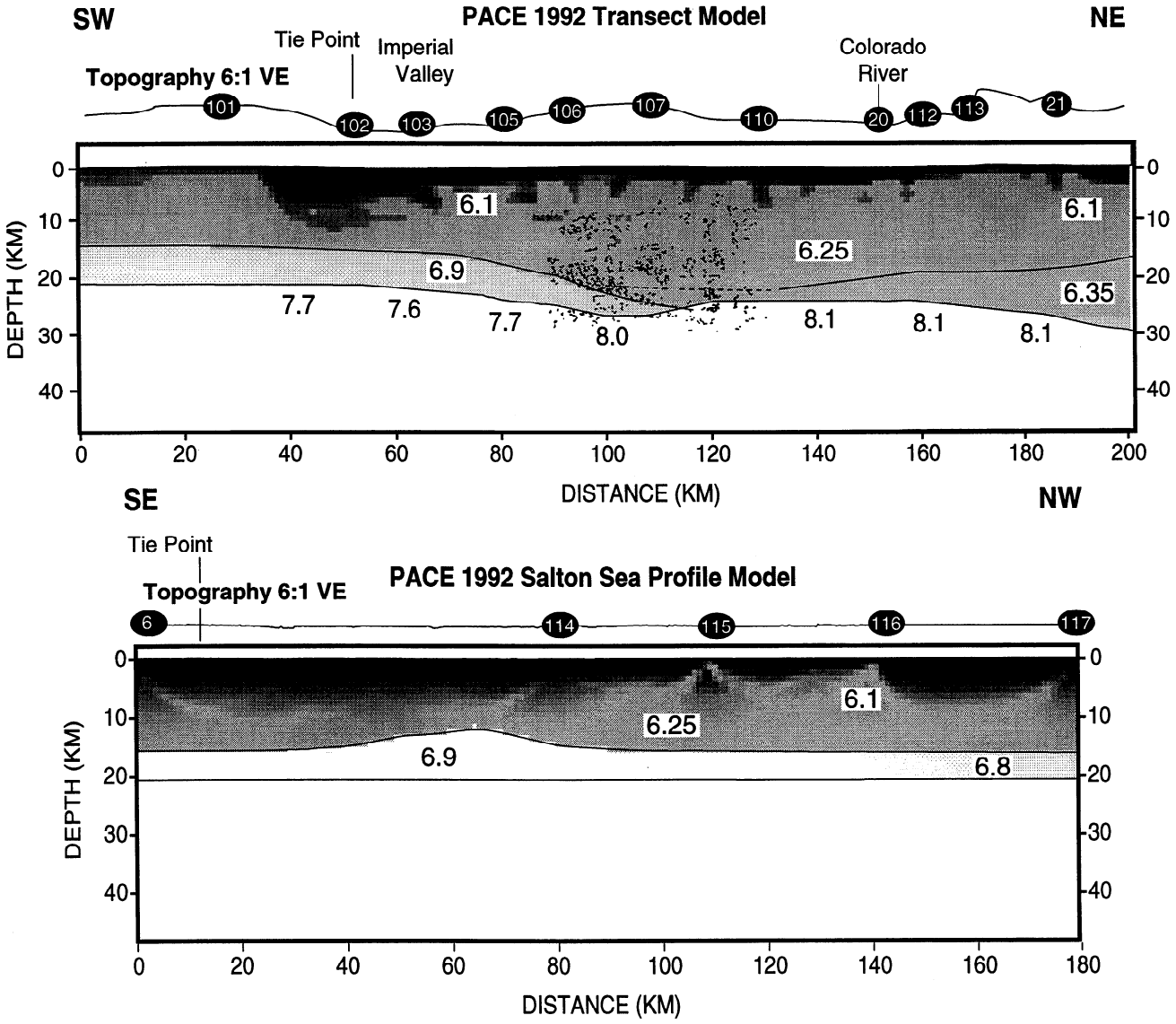

Figure 6. Crustal velocity models for the transect and Salton Sea profiles. Major features are a high-velocity (~6.9 km/s) layer at the base of the crust that pinches out beneath the Chocolate Mountains. Line drawings of the Rice University vertical incidence data (Larkin et al., submitted manuscript, 1995) are shown on the model. The dipping series of reflections that terminate at the Moho (at ~km 115 on the model) were used to determine the location and shape of the pinch-out. The presence of the high-velocity layer beneath the Salton Sea profile is an indication that this feature may be regionally present beneath the Salton Trough. Results of a travel-time inversion for upper mantle velocity structure from *Pn* arrivals on the transect profile are summarized as velocity labels at the Moho. We find relatively low upper mantle velocities (7.6-7.7 km/s) beneath the Imperial Valley-Salton Trough. Velocities increase to 8.0-8.1 km/s beneath the Chocolate Mountains. These velocities are the same as observed beneath the rest of the PACE profiles to the northeast [*McCarthy et al.*, 1991; Parsons et al., submitted manuscript, 1995]. See text for further discussion on the crustal models.

An advantage of applying finite-difference travel-time calculations was that the output gridded velocity models could be input directly into a finite-difference solution to the acoustic wave equation to simulate features of the wide-angle data. The acoustic approach simulates the Earth as a compressible fluid through which longitudinal waves propagate. While no shear waves are generated using the acoustic method, the substantial reduction in computation time and memory requirements over elastic wave equation solutions makes this approach more practical. To avoid grid dispersion (deviation between numerical and wave equation phase velocity), the input velocity grid was subsampled from a 1-km to 0.1-km grid spacing by linear interpolation. We used a source wavelet in the acoustic modelling that was extracted

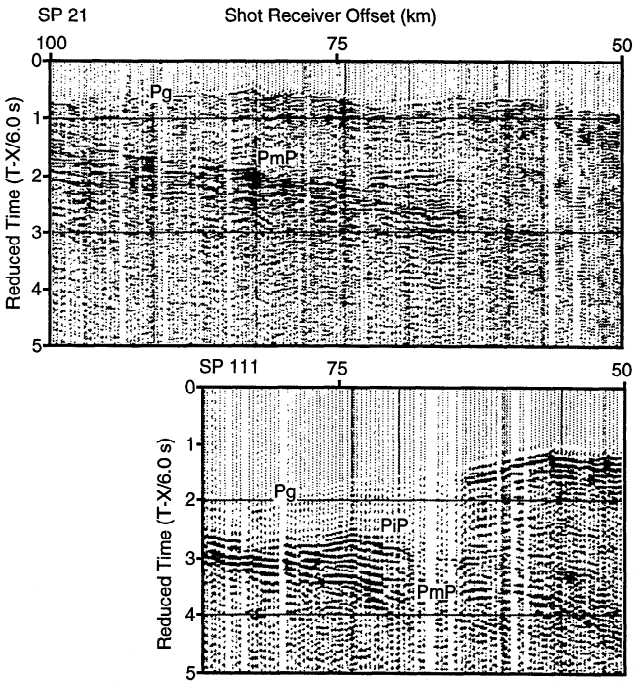

Figure 7. Examples of shots that generated reflections from the Moho (*PmP*) (shot 21, above) and from a middle crustal horizon (*PiP*) as well as the Moho (shot 111, below). The additional complexity introduced by the *PiP* reflection is apparent on sp 111 at ~75 km offset.

from the direct arrival of an explosive source on a vertical-incidence reflection spread using the same instrument types as used in collection of the wide-angle PACE data [*Parsons et al.*, 1992]).

We modelled three shots on the transect profile that bottomed southwest of the lower crustal pinch-out (shot 102, Figure 9), at the pinch-out (shot 20, Figure 10), and northeast of the pinch-out (shot 21, Figure 11). We had three goals for our amplitude modelling: (1) to test the model of the pinch-out to see if the relative complications in the wide-angle reflections could be duplicated with such a structure, (2) to establish if the velocity of 6.9 km/s assigned to the lower crustal layer generated appropriate reflection amplitudes for the middle-crustal and Moho reflections, and (3) to assess the role of upper-crustal structural complexities in the multicyclic appearance of the wide-angle reflections. A comparison of Figures 9, 10, and 11 shows that our pinch-out model does reasonably well in duplicating the relative amplitudes of the middle-crustal and Moho reflections; the shots that bottom at or southwest of the pinch-out (102, 20, Figures 9 and 10) show more complexity in the wide-angle reflections where the middle-crustal reflections interfere with or arrive just prior to the *PmP* reflections. In addition, the acoustic models show that a lower crustal velocity of 6.9 km/s is effective in generating weak middle-crustal reflections at near offsets and stronger reflections at wide angles as observed in the data; also, the model for shot 102 (Figure 9) duplicated the amplitude of the *Pn* phase as it appears on the data.

By including the complicated upper crustal model in the acoustic amplitude modelling we were able to reproduce the multicyclic appearance of the *PmP* reflections (see for example shot 102, Figure 9). This is a similar result to that of Parsons et al. (submitted manuscript, 1995) for PACE data on the Colorado Plateau. In those models, removal of the complex upper crustal velocity model greatly simplified the modelled *PmP* reflections, and the conclusion was that strong upper crustal velocity contrasts caused short-path multiples and scattering of the wide-angle reflections. We included absorbing sides and top of the velocity model so that it is

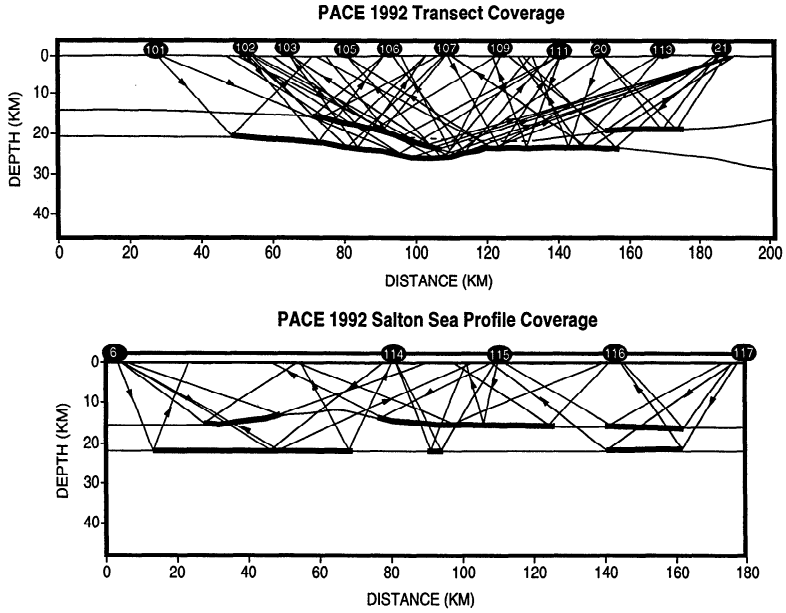

Figure 8. Reflection midpoint coverage for the middle crustal and Moho reflectors on the transect and Salton Sea profiles. The heavy lines on the reflectors mark places where the model is constrained.

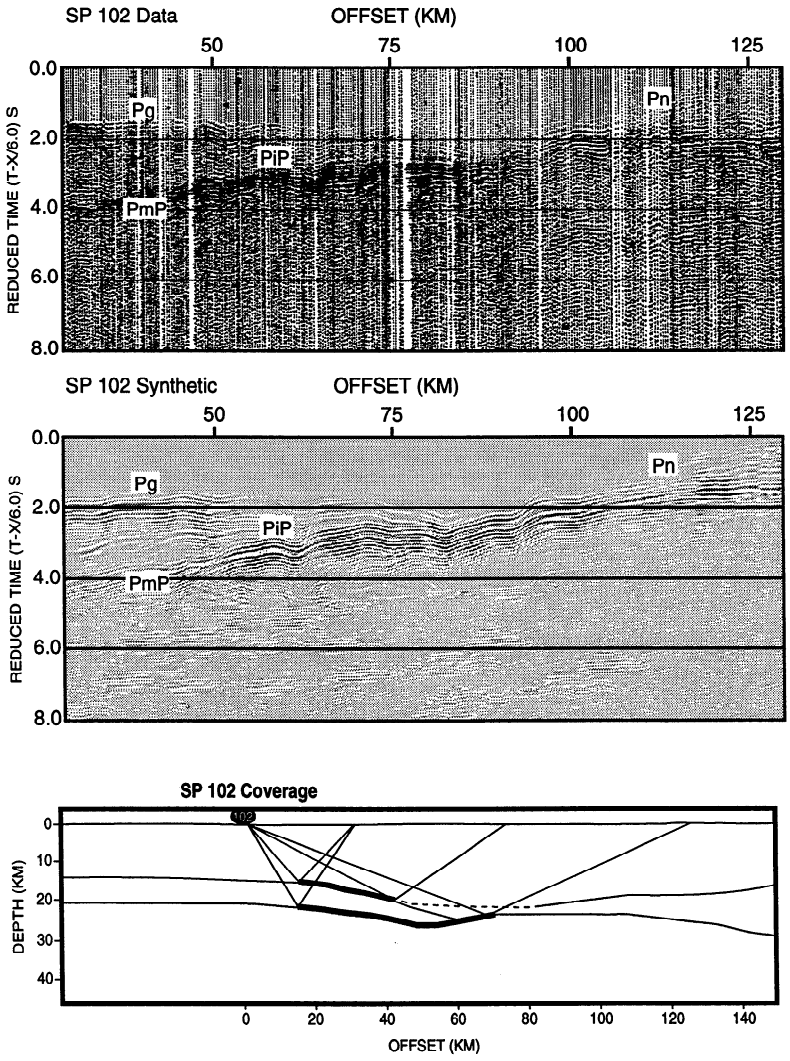

Figure 9. Results of acoustic wave equation modelling of seismic amplitudes for shot 102 on the transect profile (Figure 2). Offsets are shown from 30 km to the end of the recording spread. The model matches well the observed amplitudes of the major phases as labeled. The midpoint coverage of the reflections is shown below; energy from this shot bottoms southwest of the pinch-out of the high-velocity lower crustal layer. See text for further discussion of the amplitude modelling.

unlikely that the complications we observe in the reflections result from multiples from a free surface at the model top.

Upper Mantle Velocities From Inversion of *Pn* Arrivals

After we generated an acceptable crustal velocity model, we used it as a starting model for a travel-time inversion for upper mantle velocity structure using observed *Pn* travel times. We superimposed our crustal model on an upper mantle that had an initial uniform velocity of 8.0 km/s. We inverted 457 *Pn* travel-time observations from seven shots for upper mantle velocity structure. The results of the inversion are summarized in Figure 6. We found relatively slow (7.6-7.7 km/s) upper mantle velocities directly beneath the Salton Trough that persist to about 35 km east of the axis of the trough. We find more normal (relative to the rest of the PACE transect, [*McCarthy et al.*, 1991; Parsons et al., submitted manuscript, 1995]) upper mantle velocities of 8.0-8.1 km/s to the northeast beneath the Chocolate Mountains and the Colorado River (Figure 6). No *Pn* arrivals were recorded on the Salton Sea profile.

Error Bounds on the Analysis

Like nearly all long-offset crustal studies, our best velocity control is on the uppermost crust, where we can measure the velocity directly from the travel times of direct and refracted waves (*Pg*). The travel-time inversion for velocity converged to a solution with an RMS of 0.08 s. We estimate the maximum picking error to be 0.1 s on the PACE data. Thus the accuracy of the inversion in travel time exceeds our confidence

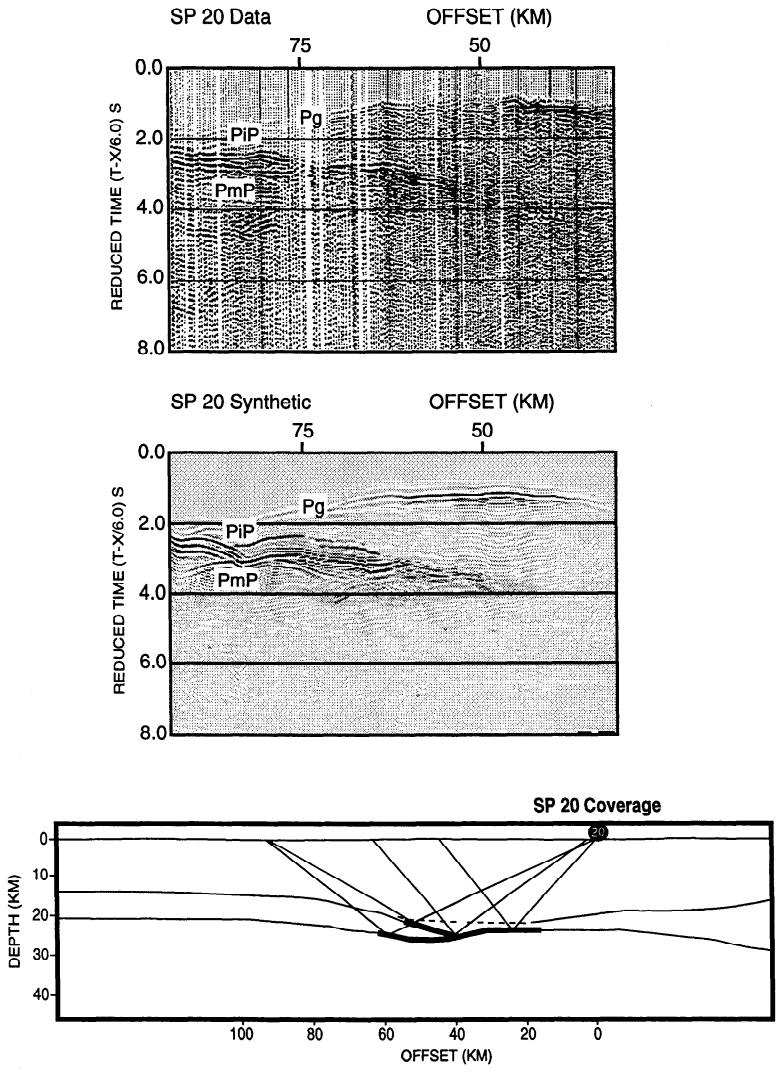

Figure 10. Results of acoustic wave equation modelling of seismic amplitudes for shot 20 on the transect profile (Figure 2). Offsets are shown from 30 km to the end of the recording spread. The midpoint coverage of the reflections is shown below; energy from this shot bottoms at the pinch-out of the high-velocity lower crustal layer.

in our picks. Because the inversion was parameterized in 0.5-km blocks, the vertical and lateral resolution is limited in an absolute sense by that spacing. The true lateral resolution is wider than 0.5 km and is limited by the Fresnel Zone width. The Fresnel Zone is calculated by computing the travel time from the source to a point in the model and then on to the receiver. At the turning depth for *Pg*, the Fresnel Zone is about 2 km wide, indicating the limit of lateral resolution. As expected, the Fresnel Zone is smaller at shallow depths where velocities are lower, and resolution should be expected to improve in these regions, provided adequate sampling by the data. Figure 3 contains the coverage matrix for the final iteration of the inversion for the transect model. The coverage for a node is calculated by summing the ray lengths of each ray path within a given cell. Thus we can resolve the shapes and velocities of upper crustal basins to ~0.5 km in the vertical dimension and ~2 km in the horizontal where sufficient ray coverage permits (Figure 3).

Error ranges in the modelled velocity structure increase with depth. Beneath ~5-to 8-km depth, the velocities in the crust are determined wholly by wide-angle reflections from the middle and lower crust. We held all residuals between observed and calculated travel times for the reflection modelling to be less than the estimated picking error of 0.1 s. Figure 12 illustrates the effects of velocity-depth perturbations from our preferred model. A 0.2 km/s increase or decrease in lower crustal velocity (combined with an appropriate decrease or increase in crustal thickness to best match observed travel times) causes unacceptable mismatches between the calculated and observed wide-angle reflection travel-time curves. We thus estimate that our resolution in velocity as determined from wide-angle reflections is $\sim\pm1$ 0.1 km/s. That velocity resolution is coupled with a $\sim\pm1.0$-km depth resolution for crustal reflecting horizons. There are local complications in structure that could be introduced to allow better fits with the faster or slower velocities for the shots depicted in Figure 12,

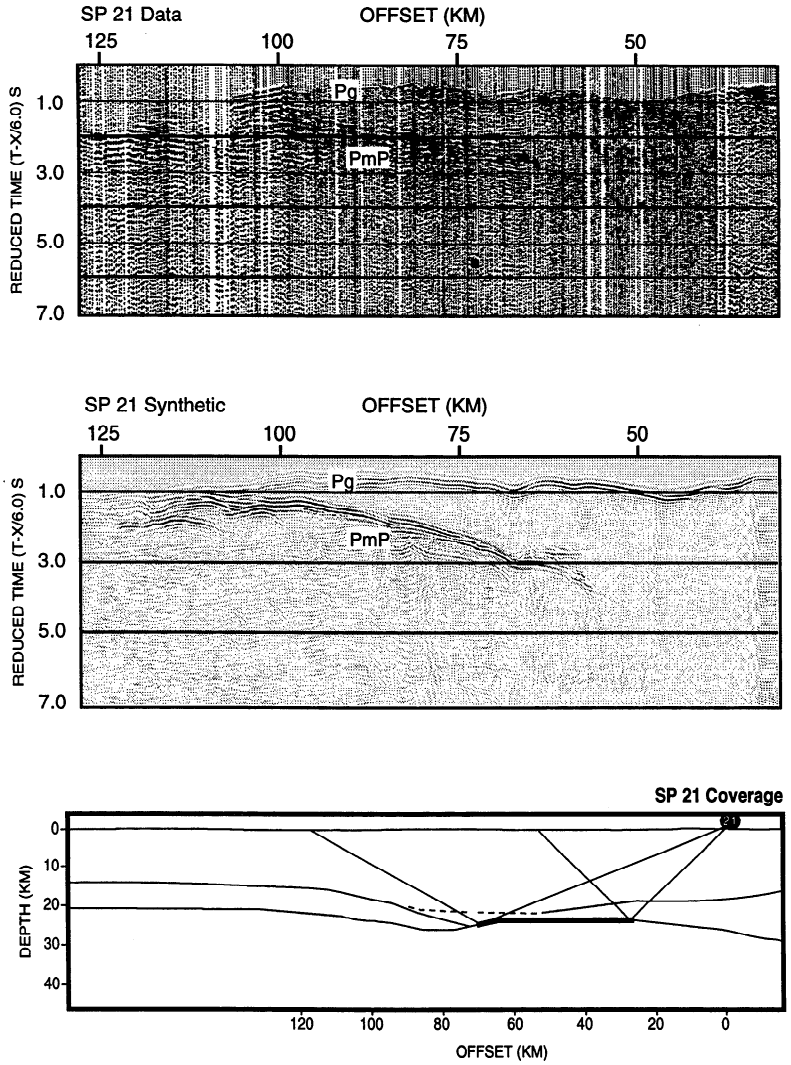

Figure 11. Results of acoustic wave equation modelling of seismic amplitudes for shot 21 on the transect profile (Figure 2). Offsets are shown from 30 km to the end of the recording spread. The midpoint coverage of the reflections is shown below; energy from this shot bottoms northeast of the pinch-out of the high-velocity lower crustal layer.

but the reversing coverage from other shots (Figure 8) precludes the introduction of such structures.

Two-Dimensional Gravity Analysis Coincident With the Seismic Models

We converted the seismic models of the transect and Salton Sea profiles to density models to ensure that they are consistent with the observed Bouguer gravity anomaly along the profiles. We did not attempt to model the detailed variations in the observed Bouguer gravity that have shallow sources but rather concentrated on the broader anomalies associated with major crustal structures (we limited fits to within 10 mGal of the observed Bouguer anomaly). The densities used by *McCarthy et al.* [1991] for modelling the PACE 1987 profile were extended into the 1992 profiles, and reasonable fits were achieved (Figures 13 and 14).

The Bouguer anomalies on both the transect and Salton Sea profiles are relatively flat. This appears to result from the deepest basins overlying the thinnest crust such that the reduction in the gravity signal from low-density sedimentary rocks is balanced by the elevation of high-density upper mantle rocks (Figure 13). We modelled a slight thickening of the crust southwest of the Imperial Valley (beneath the axis of the Salton Trough; km 50 on Figure 13) where our crustal model is unconstrained by seismic coverage. We needed to introduce some decreased density to the model there because the Imperial Valley thins to the southwest while the Bouguer anomaly remains flat (Figure 13). A lateral decrease in crustal or mantle density southwest of the Imperial Valley is also possible. At the northeast end of the transect model a decrease in the Bouguer anomaly corresponds to the crustal thickening beneath the metamorphic core complex belt. The Bouguer gravity model shown in Figure 13 includes a $\leq$10 mGal misfit

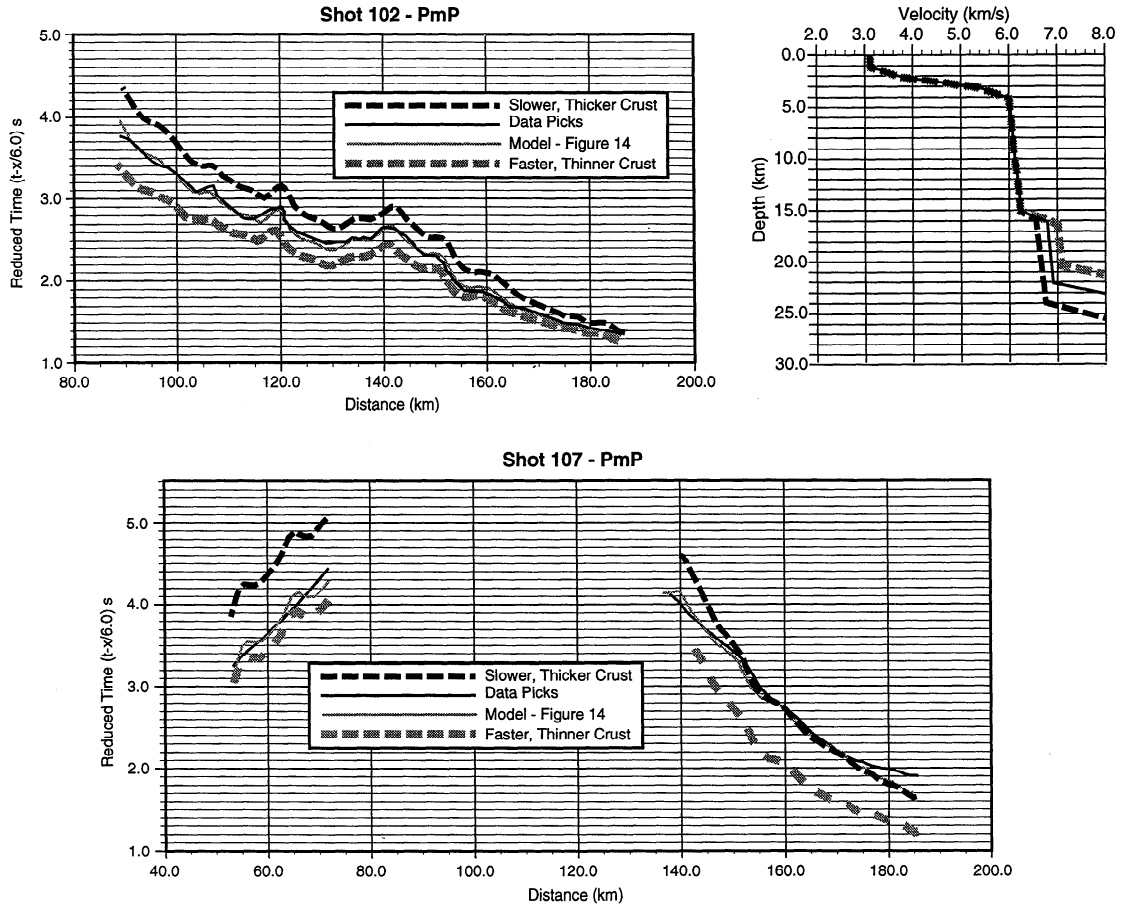

Figure 12. Examples of effects of velocity and depth perturbations in the crustal model on calculated travel-time curves for two shots (102, 107) on the transect profile. We find that detectable travel-time curvature mismatches occur if the lower crustal velocities are perturbed by more than ± 0.1 km/s or reflectors are moved by ±1 km in depth. The line weights and shading of the travel-time curves correspond to those of the velocity depth profiles shown.

across the Imperial Valley (km 20-85). We interpret much of this to be the result of very shallow, low-density sediments that were poorly resolved by the ~10-km shot spacing in our seismic models.

We generated a very simple gravity model for the Salton Sea profile which also has a nearly flat Bouguer anomaly (Figure 14). We introduced a slight thickening in the crust at the northwest end of the profile beyond the limit of seismic coverage to match the slight decrease in the Bouguer anomaly. We chose to thicken the crustal gravity model on the assumption that the crust thickens in correspondence with the increase in topographic elevation at the northwest end of the profile. There are of course many other ways to fit the subtle variation in the Bouguer anomaly such as a lateral compositional density contrast.

Discussion and Implications of the Models

A broad summary of the crustal and upper mantle models of the Salton Trough region consists of the following features: (1) a young (based on observation of velocities appropriate for unmetamorphosed sediments at depth), deep basin (~5-6 km) beneath the axis of the Salton Trough, (2) a regional deep crustal layer of 6.9 km/s velocity that is present beneath the Imperial Valley and extends ~65 km to the northeast where it pinches out beneath the Chocolate Mountains, (3) a generally thin ~20 to 22 km-thick crust beneath the Salton Trough that thickens gradually to ~27 km thick beneath the Chocolate Mountains, and (4) a low-velocity (7.6-7.7 km/s) upper mantle that occurs beneath the Salton Trough and becomes faster (~8.0-8.1 km/s) northeast of the Chocolate Mountains. These observations consistently show significant changes at all levels in the crust and upper mantle across a boundary line marked by the Chocolate Mountains. The crust and upper mantle southwest of the Chocolate Mountains have anomalous velocities relative to the rest of the PACE transect, where lower crustal velocities are closer to 6.5-6.6 km/s, upper mantle velocities are ~8.0-8.1 km/s, and no deep (> 2-3 km) upper-crustal basins are observed [e.g., *McCarthy et al.*, 1991; Parsons et al., submitted manuscript, 1995].

Our velocity model, when localized to the Salton Trough, supports a model that suggests a balanced fraction of crustal

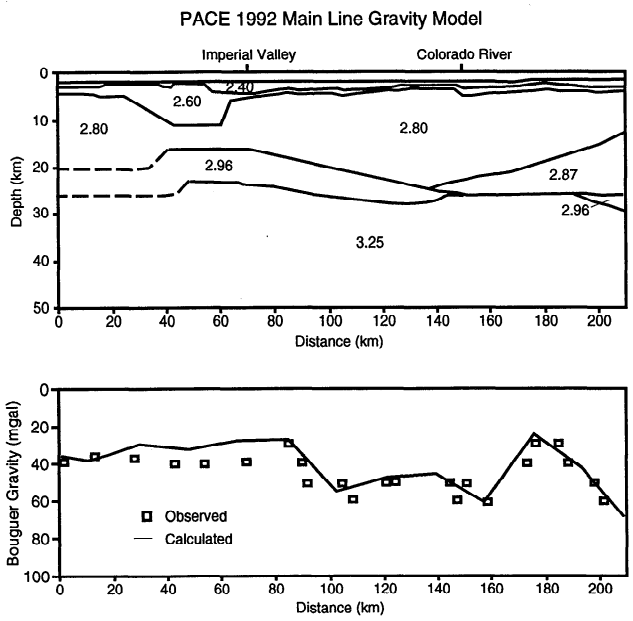

Figure 13. The crustal model of the transect profile converted to density and fit to the observed Bouguer gravity anomaly. Density boundaries are dashed where the model is not constrained by seismic coverage. See text for discussion.

replacement by active lower crustal intrusion and active upper crustal basin-forming extension (this fraction was estimated to be about 20-50% based on the thermal modelling of *Lachenbruch et al.* [1985]). Our observed lower crustal velocity of 6.9 km/s falls in the middle of the reported range of laboratory velocity measurements on gabbros corrected for depths of 15-20 km and high temperature [e.g., *Holbrook*, 1988; *Holbrook et al.*, 1992] and could be an indication of complete lower crustal formation by gabbroic intrusion. Further support for the hypothesis of mid-ocean ridge-type intrusion beneath the Salton Trough comes from modelling of the coincident vertical-incidence seismic data by Larkin et al. (submitted manuscript, 1995). Their reflection data show that crustal reflectivity is limited to the outside edges of the 6.9-km/s lower crustal layer (Figure 6), and they can model that reflectivity pattern with a series of vertical sheeted dikes forming the high-velocity layer and a small fraction (~5-20%) of intrusion of mafic sills just outside the high-velocity layer.

We observe, however, a fast (~6.9 km/s) lower crustal layer that, at the lateral resolution (~5-10 km) of wide-angle reflection modelling, appears contiguous from the axis of the trough at the Imperial Valley out to ~65 km to the northeast, where it pinches out beneath the Chocolate Mountains. If we impose a constraint that requires broad, long-term extensional strain balance in the upper and lower crust, then we would expect to see deep basins like the Imperial Valley and recent upper-crustal extension persisting into the Chocolate Mountains area if the 6.9-km/s layer represents lower crustal growth by magmatism across its full extent. The fact that such extreme post-Miocene upper crustal extension is not observed east of the Imperial Valley region despite the presence of the high-velocity layer and low-velocity upper mantle beneath the Chocolate Mountains indicates a possible lateral change in the age or origin of the high-velocity lower crust to the northeast.

There is evidence that there was probably active crustal spreading to the east of its present locus in the Imperial Valley. In figure 2, the locations of the Sand Hills, Algodones, and other Late Cenozoic transform faults are shown; these faults are thought to be fossil transforms [e.g., *Lonsdale*, 1989; R. Tosdal, personal communication, 1995] and may have offset spreading centers similar to those active southwest of the Sand Hills fault. Low-intensity geothermal systems along basement highs along the Sand Hills fault may reflect remnants of this spreading center. If this type of system was active in the past, then a mechanism for some of the apparent magmatically emplaced high-velocity lower crustal layer could be extended to about 55-60 km northeast of the axis of present-day spreading in the Salton Trough, though still about 5-10 km short of its northeast extent beneath the Chocolate Mountains. We thus must still explain the presence of this layer and apparently associated low-velocity upper mantle beneath the Chocolate Mountains region which has not been actively extending since about 11 Ma. That extensional activity in the Chocolate Mountains during Miocene time might be related to the high-velocity layer beneath them.

The isotopic signatures of surface volcanic rocks in the Salton Trough and Chocolate Mountains show that the region was broadly rifted during the Miocene and that basalts erupted at that time interacted with the lower crust, whereas basalts erupted during the most recent stages of rifting are relatively uncontaminated by the crust [*Herzig and Jacobs*, 1994]. This result was suggested to imply that much of the crust was disrupted and intruded prior to the latest rifting episode. Thus it is possible that the 6.9-km/s rocks beneath the Chocolate Mountains were emplaced during the Miocene and have no genetic link to the recent oceanic-style rifting in the Salton

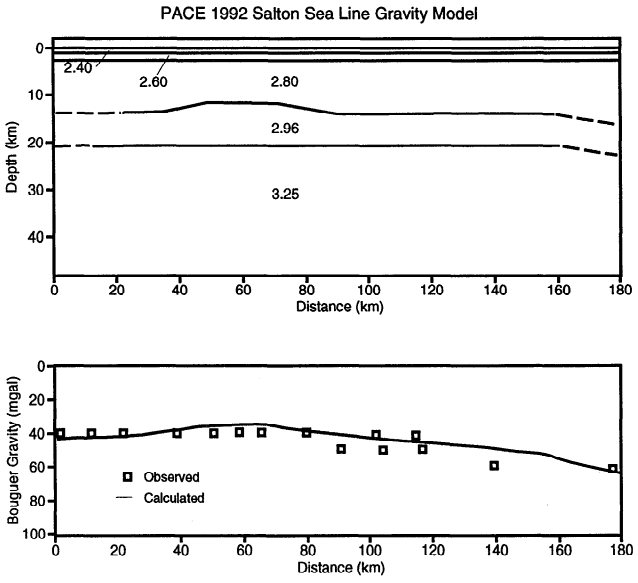

Figure 14. The crustal model of the Salton Sea profile converted to density and fit to the observed Bouguer gravity anomaly. Density boundaries are dashed where the model is not constrained by seismic coverage. See text for discussion.

Trough. The upper mantle beneath the Chocolate Mountains is, however, anomalously slow at 7.6-7.7 km/s to have been inactive since the middle Miocene; such low velocities suggest a state of partial melt. It thus seems likely that the upper mantle anomaly related to Salton Trough rifting is much broader than the width of the surface rift, an observation supported by tomographic inversions of teleseismic residuals in southern California [*Humphreys and Clayton*, 1990] that show a broad, asymmetric low-velocity upper mantle anomaly beneath the Salton Trough.

We conclude that the high-velocity layer that extends beneath the Chocolate Mountains results from Miocene or older intrusions related to broad Basin and Range style rifting and a spatially variable amount of more recent intrusion related to the northward migration of mid-ocean spreading in the Gulf of California. An estimated 240 km of right slip occurred on the southern San Andreas fault system between 5 Ma and the present [*Dillon and Ehlig*, 1993], and that amount of lower crust may have been created at localized magmatic spreading centers where the southern end of the San Andreas system was offset. Thermal modelling and surface/marine geology indicate that these spreading-center offsets at the southern end of the San Andreas system have been mobile and possibly short-lived [e.g., *Lachenbruch et al.*, 1985; *Lonsdale*, 1989; *Larsen and Reilinger*, 1991]. Such continued spreading-center realignment has either caused, or has been caused by, a broad upper mantle thermal anomaly that has allowed intrusion into the lower crust in equal proportion to the amount of surface rifting. In places where spreading centers have been stable for relatively long periods of time, new crust has been created by a combination of magmatism and sedimentation [e.g., *Fuis et al.*, 1984; *Lachenbruch et al.*, 1985; *Nicolas*, 1985]. In places where spreading centers may have been more ephemeral, the lower crust may have been less intruded and surface extension less recognizable.

Conclusions

A crustal and upper mantle seismic transect across the Salton Trough region revealed the following features: (1) in the upper crust, a young, deep (~5-6 km) basin beneath the axis of the Salton Trough at the Imperial Valley, a shallower (~2-3 km deep) basin beneath the Colorado River, and an intervening basement uplift beneath the Chocolate Mountains; (2) a regional high-velocity (6.9 km/s) layer occurs between ~15-km depth and the base of the crust that is apparently intruded by mafic igneous rocks; this layer is present beneath the Salton Trough and pinches out at the Moho ~65 km northeast of the rift axis beneath the Chocolate Mountains; (3) the crust is ~21-22 km thick beneath the axis of the Salton Trough, thickens to ~27 km beneath the Chocolate Mountains, thins to about 24 km beneath the Colorado River, and then begins to thicken again to the northeast beneath the metamorphic core complex belt; and (4) the upper mantle is slow (7.6-7.7 km/s) beneath the Salton Trough, and low-velocity upper mantle extends northeast beneath the Chocolate Mountains where it speeds up to 8.0-8.1 km/s. These crustal and upper mantle features formed as a result of two phases of extension, a broad Basin and Range style episode during the Miocene and a later, still active phase of ocean basin rifting. In the central axis of the Salton Trough, new crust has formed by combination of magmatism from below and sedimentation from above. To the northeast beneath the Chocolate Mountains, despite the continued presence of the 6.9-km/s lower crustal layer, it appears that the whole crust has been less severely influenced by the latest stages of oceanic-style spreading. We propose a model where the loci of crustal spreading centers have migrated and probably were located east of their present configuration in the past and were less evolved than the currently active centers; this may have caused some intrusion into the lower crust and may be related to the broader zone of anomalous upper mantle relative to the breadth of surface rifting.

Acknowledgments. We especially acknowledge Chuck Ammon, Harley Benz, Ed Criley, Gordon Haxel, Dick Tosdal, and Gene Wissenger for invaluable assistance during the planning, collection, and analysis phases of this study. We wish to extend a special thank you to Tim Cartwright, Tim Coté, Marcel Gervais, and the Geological Survey of Canada for the use of the Canadian refraction instruments during this investigation. We thank Steve Larkin for providing reflection data plots. We thank Chuck Ammon and John Hole for providing the data analysis code used in this study. Steve Larkin, Art Sylvester, Uri ten Brink, and Dick Tosdal provided very helpful review comments on the manuscript. The U.S. Geological Survey's Deep Continental Studies Program provided funding for this project.

References

Ammon, C. J., and J. E. Vidale, Tomography without rays, *Bull. Seismol. Soc. Am.*, 83, 509-528, 1993.

Crowe, B. M., Cenozoic volcanic geology and probable age of inception of basin-range faulting in the southeasternmost Chocolate Mountains, California, Geol. Soc. Am. Bull., 89, 251-264, 1978.

Crowell, J. C., Sedimentation and tectonics along the San Andreas transform belt, in *Sedimentation and Tectonics of North America,* Volume 2, *The San Andreas Transform Belt, Field trip Guideb.*, vol. T309, edited by A. G. Sylvester and J. C. Crowell, pp. 32-35, AGU, Washington D. C., 1989.

Dillon, J. T., and P. L. Ehlig, Displacement on the southern San Andreas fault, in *The San Andreas Fault System: Displacement, Palinspathic Reconstruction, and Geologic Evolution,* edited by R. E. Powell, R. E. Weldon, and J. C. Matti, *Mem. Geol. Soc. Am., 178,* 199-216,1993.

Elders, W. A., R. W. Rex, T. Meidav, P. T. Robinson, and S. Biehler, Crustal spreading in southern California, *Science, 178*, 15-24, 1972.

Fuis, G. S., W. D. Mooney, J. H. Healy, G. A. McMechan, and W. J. Lutter, A seismic refraction survey of the Imperial Valley Region, California, *J. Geophys. Res., 89,* 1165-1189, 1984.

Herzig, C. T., and D. C. Jacobs, Cenozoic volcanism and two-stage extension in the Salton trough, southern California and northern Baja California, *Geology, 22*, 991-994, 1994.

Holbrook, W. S., Wide-angel seismic studies of crustal structure and composition in Nevada, California, and southwest Germany, Ph.D. thesis, 214 pp., Stanford Univ., Stanford, Calif.., 1988.

Holbrook, W. S. W. D. Mooney, and N. I. Christensen, The seismic velocity of the deep continental crust, in *Continental Lower Crust* edited by D. M. Fountain, R. Arculus, and R. Kay, pp. 1-43, Elsevier, New York, 1992.

Hole, J. A., Structure of the Queen Charlotte basin and underlying crust from modelling and inversion of three-dimensional seismic refraction data, Ph.D. thesis, 144 pp., Univ. of British Columbia, Vancouver, B. C., Canada, 1993.

Hole, J. A., and B. C. Zelt, 3-D finite-difference reflection travel times, *Geophys. J. Int., 121*, 427-434, 1995.

Humphreys, E. D., and R. W. Clayton, Tomographic image of the southern California mantle, *J. Geophys. Res., 95*, 19,725-19,746, 1990.

Korsch, R. J., Cenozoic volcanic activity in the Salton Trough region, in *Tectonics of the Juncture Between the San Andreas Fault System and the Salton Trough, Southeastern California,* edited by J. C. Crowell and A. G. Sylvester, pp. 87-101, Dep. of Geol. Sci., Univ. of Calif. Santa Barbara, 1979.

Lachenbruch, A. H., J. H. Sass, and S. P. Galanis, Heat flow in southernmost California and the origin of the Salton Trough, *J. Geophys. Res., 90*, 6709-6736, 1985.

Larsen, S., and R. Reilenger, Age constraints for the present fault configuration in the Imperial Valley, California: Evidence for northwestward propagation of the Gulf of California rift system, *J. Geophys. Res., 96*, 10,339-10,346, 1991.

Larson, P. A., H. W. Menard, and S. M. Smith, Gulf of California: A result of ocean-floor spreading and transform faulting, *Science, 161*, 781-784, 1968.

Lonsdale, P., Geology and tectonic history of the Gulf of California, in *The Geology of North America,* vol. N, *The Eastern Pacific Ocean and Hawaii,* edited by E. L. Winterer, D. M. Hussong, and R. W. Decker, pp. 499-521, Geol. Soc. Am., Boulder, Colo., 1989.

McCarthy, J., and T. Parsons, Kinematic model for the Cenozoic evolution of the Colorado Plateau - Basin and Range transition from coincident seismic refraction and reflection data: *Geol. Soc. Am. Bull., 106*, 747-759, 1994.

McCarthy, J., S. P. Larkin, G. S. Fuis, R. W. Simpson, and K. A. Howard, Anatomy of a metamorphic core complex: Seismic refraction/wide-angle reflection profiling in southeastern California and western Arizona, *J. Geophys. Res., 96*, 12,259-12,291, 1991.

Moore, D. G., and E. C. Buffington, Transform faulting and the growth of the Gulf of California since late Pliocene, *Science, 161*, 1238-1241, 1968.

Nicolas, A., Novel type of crust produced during continental rifting, *Nature, 315*, 112-115, 1985.

Parsons, T., J. M. Howie, and G. A. Thompson, Seismic constraints on the nature of lower crustal reflectors beneath the extending southern Transition Zone of the Colorado Plateau, Arizona, *J. Geophys. Res., 97*, 12391-12407, 1992.

Powell, R. E., Balanced palinspathic reconstruction of pre-late Cenozoic paleogeology, southern California: Geologic and kinematic constraints on evolution of the San Andreas fault system, in *The San Andreas Fault System: Displacement, Palinspathic Reconstruction, and Geologic Evolution,* edited by R. E. Powell, R. E. Weldon, and J. C. Matti, *Mem. Geol. Soc. Am., 178*, 1-106, 1993.

Stock, J. M., and K. V. Hodges, Pre-Pliocene extension around the Gulf of California and the transfer of Baja California to the Pacific Plate, *Tectonics, 8*, 99-115, 1989.

Swanberg, C. A., Geothermal resources of rifts: A comparison of the Rio Grande rift and the Salton Trough, *Tectonophysics, 94*, 659-678, 1983.

Vidale, J. E., Finite-difference calculation of traveltimes, *Bull. Seismol. Soc. Am., 78*, 2062-2076, 1988.

Vidale, J. E., Finite-difference calculation of traveltimes in three dimensions, *Geophysics, 55*, 521-526, 1990.

Wilson, J. M., and G. S. Fuis, *Data report for the Chemehuevi, Vidal, and Dutch Flat lines: PACE seismic-refraction survey, southeastern California, and western Arizona, U.S. Geol. Surv. Open File Rep., 87-86,* 75 pp., 1987.

Wilson, J. M., J. McCarthy, R. A. Johnson, and K. A. Howard, An axial view of a metamorphic core complex: Crustal structure of the Whipple and Chemehuevi Mountains, southeastern California, *J. Geophys. Res., 96*, 12,293-12,311, 1991.

Wolf, L. W., and J. J. Cipar, The Colorado Plateau through thick and thin, *J. Geophys. Res., 98*, 19,881-19,894, 1993.J.

McCarthy and T. Parsons, U. S. Geological Survey, Branch of Pacific Marine Geology, Mail Stop 999, 345 Middlefield Road, Menlo Park, CA 94025.
(email: tparsons@octopus.wr.usgs.gov)

(Received March 14, 1995;
revised August 16, 1995;
accepted August 17, 1995.)